

THE LAST GLACIAL MAXIMUM CLIMATE OVER THE LAURENTIDE ICE SHEET:
HIGH-RESOLUTION SIMULATIONS USING POLAR MM5

David H. Bromwich^{1,2}, E. Richard Toracinta¹, Robert Oglesby³, Helin Wei⁴, James Fastook⁵, and Terence Hughes⁵

¹Polar Meteorology Group, Byrd Polar Research Center, The Ohio State University

²Atmospheric Sciences Program, Department of Geography, The Ohio State University

³NASA Marshall Space Flight Center/ National Space Science and Technology Center

⁴National Centers for Environmental Prediction

⁵Institute for Quaternary and Climate Studies, University of Maine

1. INTRODUCTION

In the effort to better understand possible climate change mechanisms, particular attention has been focused on the Last Glacial Maximum (LGM) roughly 21,000 calendar years before present (21 kBP; Mix et al. 2001). During this period, the Laurentide and Fennoscandian ice sheets covered much of North America and Scandinavia, respectively, and the global climate was much colder than present. Climate modelers in particular have benefited from the relative abundance of proxy data available from the LGM that provide boundary conditions for atmospheric global climate model (GCM) simulations. Many such studies of the global LGM climate have been conducted (e.g., Kutzbach and Guetter 1986; Rind 1987; Wright et al. 1993; Pollard and Thompson 1997; Kutzbach et al. 1998).

While individual modeling efforts have been useful for providing insight into the many important climatological consequences of Northern Hemisphere ice sheets, the results have varied substantially among the studies (Kageyama et al. 1998). The Paleoclimate Modeling Intercomparison Project (PMIP; Joussaume and Taylor 1995) combines the results of different models into a more coherent pattern. One finding of PMIP is that model resolution has a significant impact on the simulations, with the higher horizontal resolution models producing more consistent results (Kageyama et al. 1998). Simulations of the modern polar climate show a similar dependence on resolution (Tzeng et al. 1993; Chen et al. 1995). However, even at the finest resolution (2.8° lat/lon grid) commonly available, GCMs are generally unable to capture important mesoscale processes associated with large ice sheets (e.g., katabatic winds).

Regional atmospheric models, with high spatial resolution and multiple options for physical parameterizations, are being more commonly used for climate applications. Foremost among these models is the Polar MM5, a version of the Pennsylvania State University (PSU) / National Center for Atmospheric Research (NCAR) fifth-generation mesoscale model (MM5; Dudhia 1993; Grell et al. 1994) modified specifically for simulations over polar regions (Bromwich et al. 2001). The Polar MM5 has been tested extensively over present-day Greenland

(Bromwich et al. 2001; Cassano et al. 2001) and Antarctica (Bromwich et al. 2003; Guo et al. 2003) and shown to have generally minimal bias. Hence, the Polar MM5 is well suited for simulations over the Laurentide Ice Sheet, which at the LGM had spatial dimensions similar to present-day Antarctica.

In the present study, Polar MM5 is coupled to the NCAR Community Climate Model version 3 (CCM3; Kiehl et al. 1998) for simulations of the LGM climate over the Laurentide Ice Sheet. Boundary conditions include 21-kBP orbital forcing, trace gases, and vegetation, lowered sea level, and a modified version of the Climate/Long-range Investigation, Mapping, and Prediction (CLIMAP 1981) sea surface temperatures (SSTs) based on proxy data (Toracinta et al. 2003). The objective is to assess the detailed atmospheric state over the Laurentide Ice Sheet to adequately quantify the temperature, precipitation, and flow regimes that contribute to ice sheet growth and ablation.

Section 2 briefly describes the Polar MM5, the LGM boundary conditions, and the approach used for the model experiments. Section 3 compares results of one-month LGM simulations from the regional Polar MM5 and the global CCM3. Concluding statements are given in Section 4.

2. MODELS AND EXPERIMENTAL DESIGN

The Polar MM5 used in the current study is based on the standard release MM5 version 3.4 and features several modifications to optimize model performance over polar regions. These include: implementation of the Meyers et al. (1992) ice nuclei concentration equation to correct a large positive bias in the polar cloud amount; improved treatment of cloud/radiation interaction using predicted cloud water and ice; optimal treatment of boundary layer fluxes via the 1.5 order turbulence closure parameterization (Janjić 1994); increased number of soil substrate levels and depth to more accurately resolve heat transfer; improved treatment of thermal properties of ice and snow surface types (following Yen 1981); and implementation of a variable sea ice thickness and open water fraction.

The Polar MM5 LGM simulations are run at a 60-km grid interval over a 10,200-km x 9600-km domain centered over North America (Fig. 1). There are 29 vertical sigma levels and the model top is set to 13 hPa to minimize surface pressure anomalies resulting from vertically propagating gravity waves generated by steep terrain slopes (Guo et al. 2003). The Grell

Corresponding author: Dr. David H. Bromwich, Byrd Polar Research Center, 1090 Carmack Road, The Ohio State University, Columbus, OH, 43210-1002. Email: bromwich@polarmet1.mps.ohio-state.edu

cumulus parameterization and Reisner microphysics option are used in all simulations.

The Laurentide and Fennoscandian ice sheet elevation data were implemented from glaciological model output and sea level was lowered by 120 m commensurate with the LGM ice sheet volume. Since glaciological models tend to build too much ice in Alaska at the LGM, the Alaska glacier extent was implemented according to reconstructed boundaries (Manley and Kaufmann 2002) and the elevations set to present day values (i.e., zero thickness glaciers). The solar forcing was computed from 21 kBP orbital parameters (Berger 1977) and the CO₂ concentration was set to 180 ppm, consistent with data from the Vostok ice core (Petit et al. 1999). Land use types were selected from among the 13 PSU/NCAR land use categories that best matched LGM vegetation reconstructions (e.g., Williams et al. 2000).

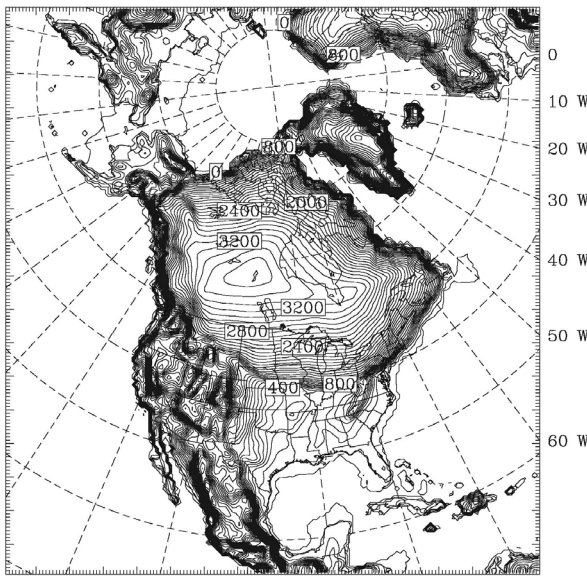


Figure 1. Polar MM5 domain and LGM terrain elevation. Contour interval is 100 m. Tick marks denote horizontal grid spacing.

The Polar MM5 simulations are one-month continuous runs preceded by a 2-week spin-up that is discarded. The initial and lateral boundary conditions are from the final year of an 18-year CCM3 LGM simulation. With the exception of modern vegetation and modified CH₄ levels in the CCM3 LGM run, the boundary conditions were identical to those used in the regional model runs. In each month-long Polar MM5 simulation, lateral boundary conditions are updated every 12 hours. Model output is every 6 hours from which monthly averages are computed.

3. LGM RESULTS

While a full annual cycle has been completed for the LGM, we present here Polar MM5/CCM3 comparisons for the extreme months, January and June.

a. January

The CCM3 LGM simulation produces a uniform westerly flow pattern over North America as indicated by the mean January¹ 500-hPa geopotential heights (Fig. 2). The mid-tropospheric circulation pattern shows a low-amplitude ridge in western North America (windward of the Laurentide Ice Sheet) and a pronounced trough axis downstream along eastern North America. The large 500-hPa geopotential height gradient in the eastern portion of the domain is indicative of a vigorous trans-Atlantic jet stream.

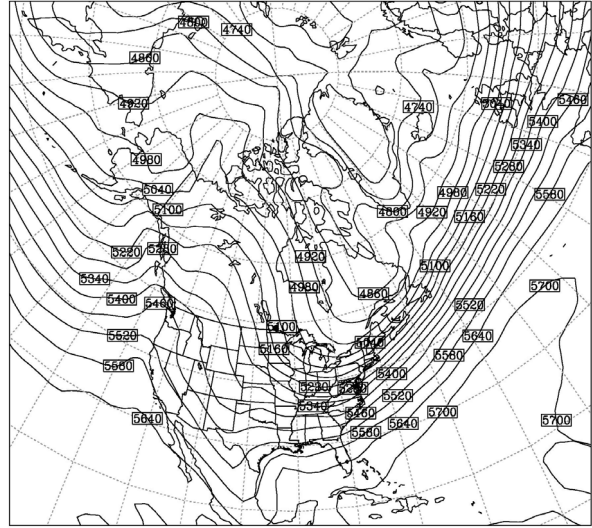


Figure 2. CCM3 LGM mean January 500-hPa geopotential height. Contour interval is 60 m.

By comparison, Polar MM5, which again is tied to the CCM3 solution only on the lateral boundaries, produces a markedly different solution (Fig. 3). Here, the mean January 500-hPa geopotential height field clearly indicates split mid-tropospheric flow over the Laurentide Ice Sheet. The circulation pattern is more highly amplified in Polar MM5 than CCM3, with a large blocking anticyclone on the windward side of the Laurentide Ice Sheet. As a result, trans-Pacific storm systems are forced either northeastward over Beringia and into the Arctic, or move across the present-day southwestern U.S. The intensity and orientation of the downstream trough is also very different in Polar MM5. The large 500-hPa geopotential height gradient over the Canadian Arctic is indicative of strong, cold northwesterly flow over the region. The split flow pattern in the Polar MM5 LGM simulation is a seasonal phenomenon that becomes established in October, is most pronounced in January, and persists through April. The inter-annual variability in the CCM3 LGM run is much less pronounced. The differences between Polar MM5 and CCM3 simulated January upper-level flow patterns point to distinct differences in the

¹ Data are from the same month/year that was used to initialize the Polar MM5 January simulation.

distribution of precipitation (accumulation) and temperature (ablation) over the Laurentide Ice Sheet.

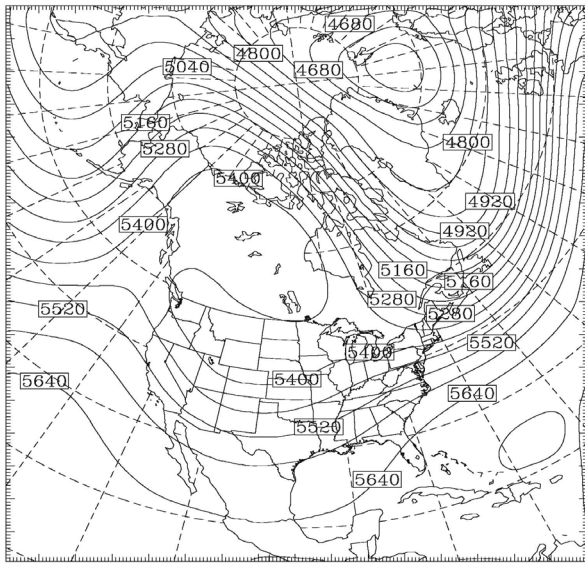


Figure 3. As in Fig. 2, but for Polar MM5.

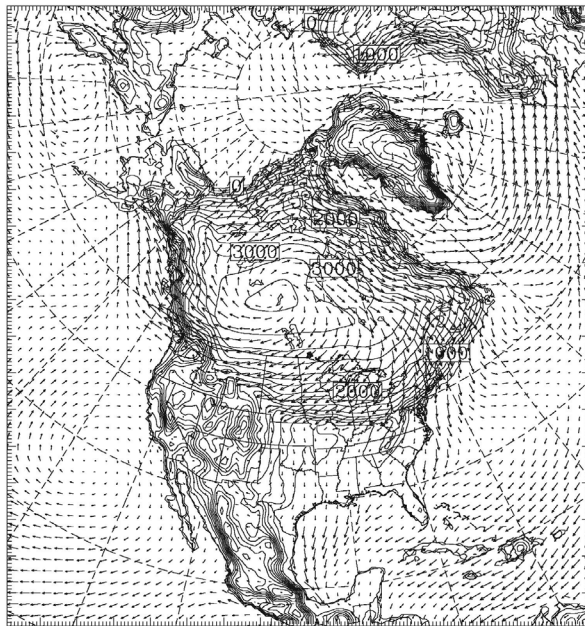


Figure 4. Polar MM5 LGM terrain elevation and mean January near-surface vector wind. Terrain contour interval is 250 m. Maximum wind vector length is 28 m s^{-1} .

Near the surface, Polar MM5 produces a pronounced anticyclone over the Laurentide Ice Sheet with mean January katabatic wind speeds exceeding 25 m s^{-1} along the ice sheet margins (Fig. 4). It must be noted that Polar MM5 tends to underestimate wind speeds during peak katabatic wind events over contemporary Antarctica (Guo et al. 2003). Thus, the monthly mean katabatic wind speeds over the

Laurentide Ice Sheet are also probably slightly underestimated. The CCM3 mean January near-surface wind speeds over the Laurentide Ice Sheet are roughly 65% weaker and there is little indication of a katabatic circulation (not shown).

The anticyclonic circulation over the ice sheet and the split flow pattern in Polar MM5 are evident through the depth of the troposphere and are clearly related to the presence of the Laurentide Ice Sheet. Using a simplified coupled ice sheet-stationary wave model, Roe and Lindzen (2001) show that continental ice sheet topography exerts a primary influence on the stationary wave pattern, which in turn determines the patterns of temperature and precipitation over the ice sheet. The authors note a high pressure centered on the western flank of the ice sheet with northerly flow downstream, broadly similar to our results in Fig. 3.

b. June

Roe and Lindzen (2001) also point out the need for added model complexity to better represent and quantify, for instance, the thermal influence of the ice sheet on the atmosphere, the feedback between transient eddies and the stationary wave pattern, and moisture source regions for ice sheet accumulation. Essentially, the need exists for a better model representation of the processes that contribute to ice sheet mass balance. The Polar MM5 is sufficiently complex to address these questions in detail. For instance, Fig. 5 shows time series from Polar MM5 of 2-meter temperature, near-surface meridional wind speed, and accumulated precipitation output every 3-hours during the final two weeks of June at a grid point on the southern margin of the Laurentide Ice Sheet (elevation 1099 m, ice thickness 886 m) in present-day central Illinois. Also plotted is the probability of liquid precipitation determined from an objective analysis of the vertical temperature structure of the model atmosphere (Bocchieri 1980).

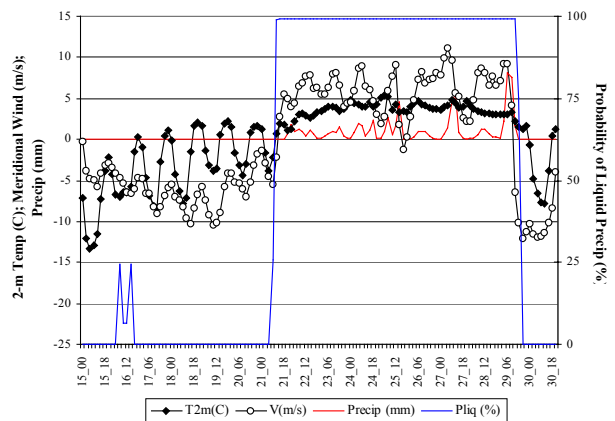


Figure 5. Polar MM5 LGM 00Z/15–21Z/30 June 3-hourly time series of 2-meter temperature ($^{\circ}\text{C}$; filled diamonds), meridional wind speed (m s^{-1} ; open circles), 3-hr accumulated precipitation (mm; red line), and probability of liquid precipitation (blue line). Grid point

location is 41°N, 89°W, 1099 m above modern sea level.

The diurnal cycle is evident in the Polar MM5 2-meter temperature and meridional wind during the initial six day period (00Z/15–00Z/21), which is mostly precipitation-free. Near-surface winds are directed downslope on the ice sheet and daytime temperatures peak slightly above freezing. Over the following eight days the flow regime changes under the influence of synoptic-scale storm systems that form along the strong baroclinic zone between the cold air mass over the Laurentide ice sheet and the adjacent warm land surface and move across the ice sheet southern margin. As a result, the near-surface winds are upslope at 5–10 m s⁻¹ drawing low-level moisture from the Gulf of Mexico, 2-meter temperatures remain above freezing, and precipitation (almost certainly rain) occurs at this location on the southern margin. With clouds and precipitation, the diurnal temperature variation is strongly damped in comparison with the preceding 6 days. The 8-day precipitation total at this site is 70 mm (approximately 2.75 inches) liquid water, some of which is convective precipitation (i.e., model thunderstorms) on the Laurentide Ice Sheet. Several such events occur on the southern margin of the ice sheet through the summer months and are a potentially important source of water to lubricate the ice sheet bed along the southern margin.

It should also be noted that, with a fixed ice sheet albedo (0.8), Polar MM5 does not capture the albedo fluctuations typically observed the ablation zone of contemporary ice sheets (e.g., Greenland) during the melt season. Snow age and grain size, impurities, snow depth, and accumulated melt can lower the surface albedo by 10–40% or more. Along the ablation zone in summer, the fixed albedo in Polar MM5 leads to errors in the modeled net radiation (Cassano et al. 2001). Hence, the 2-m air temperatures (and ice sheet melt rates) in Fig. 5 are mostly certainly under-predicted. Incorporating an evolving albedo parameterization (e.g., Box 2003) in Polar MM5 would give a more accurate representation of the southern margin albedo during the ablation season and allow for explicit calculation of surface melt.

Our initial analysis of CCM3 data for the same time period and location indicates that the global model produces a somewhat different solution. As in Fig. 5, the CCM3 indicates warm advection and probable rain on the ice sheet southern margin (not shown). However, there are substantial differences in magnitude between the two model predictions that may be attributed to the parameterizations used, the specified land surface, and the ability of the model to properly adjust to the strong temperature and moisture gradients that exist along the ice sheet margin in the warm season. Further investigation of the sensitivity of the solution to model parameterizations and land surface configurations are underway.

4. CONCLUSIONS

The atmospheric circulation features apparent in mean January and June results from LGM simulations

over the Laurentide Ice Sheet indicate that the high-resolution Polar MM5 is more sensitive to the boundary (ice sheet) forcing than the CCM3 global climate model. Polar MM5, which is optimized for simulations over continental ice sheets, simulates greater interannual variability than CCM3 on synoptic and regional scales. This has direct implications for explicit mass balance computations for the Laurentide Ice Sheet and its feedback to the climate system. It also provides a potential framework within which various proxy data methods can be tested and refined.

Roe and Lindzen (2001) note that the most important feedback from the atmospheric standing wave pattern to the ice sheet are the summer temperature distribution and topographically induced precipitation. Our analysis of high-resolution Polar MM5 output further indicates that synoptic variability in the warm season (June–September) is primarily responsible for the temperature, wind, and precipitation patterns that contribute to ablation on the Laurentide Ice Sheet margins and are not always captured in climatological mean fields.

ACKNOWLEDGMENTS. The Laurentide Ice Sheet research project is sponsored by NSF grant OPP-9905381 to D. H. Bromwich. Use of computer resources at NCAR and the Ohio Supercomputing Center was provided through grants 36091009 and PAS0045-1, respectively. Special thanks to Rahul George and Raghavendra Mupparthy for data processing assistance.

REFERENCES

- Berger, A., 1977: Long-term variations of the earth's orbital elements. *Celes. Mech.*, **15**, 53–74.
- Bocchieri, J. R., 1980: The objective use of upper air soundings to specify precipitation type. *Mon. Wea. Rev.*, **108**, 596–603.
- Box, J., 2003: Albedo parameterization in the Polar MM5 regional atmospheric circulation model. Byrd Polar Research Center Tech. Report 2003-01, 5 pp.
- Bromwich, D.H., J.J. Cassano, T. Klein, G. Heinemann, K.M. Hines, K. Steffen and J.E. Box, 2001: Mesoscale modeling of katabatic winds over Greenland with the Polar MM5. *Mon. Wea. Rev.*, **129**, 2290–2309.
- Bromwich, D.H., A.J. Monaghan, J.J. Powers, J.J. Cassano, H. Wei, Y. Kuo, and A. Pellegrini, 2003: Antarctic Mesoscale Prediction System (AMPS): A case study from the 2000/2001 field season. *Mon. Wea. Rev.*, **131**, 412–434.
- Cassano, J.J., J.E. Box, D.H. Bromwich, L. Li, and K. Steffen, 2001: Evaluation of Polar MM5 simulations of Greenland's atmospheric circulation. *J. Geophys. Res.*, **106**, 33867–33890.
- Chen, B., D.H. Bromwich, K.M. Hines, and X. Pan, 1995: Simulations of the 1979–1988 polar climates by global climate models. *Annals Glaciol.*, **21**, 83–90.
- CLIMAP Project Members, 1981: *Seasonal Reconstruction of the Earth's Surface at the Last*

- Glacial Maximum.*, Geolog. Soc. Amer. Map and Chart Series, Vol. 36, 18.
- Dudhia, J., 1993: A nonhydrostatic version of the Penn State-NCAR Mesoscale Model: Validation tests and simulation of an Atlantic cyclone and cold front. *Mon. Wea. Rev.*, **121**, 1493-1513.
- Grell, G.A., J. Dudhia and D.R. Stauffer, 1994: A description of the fifth-generation Penn State-NCAR Mesoscale Model (MM5). NCAR Tech. Note NCAR/TN-398+STR, 122 pp.
- Guo, Z., D.H. Bromwich and J.J. Cassano, 2003: Evaluation of Polar MM5 simulations of Antarctic atmospheric circulation. *Mon. Wea. Rev.*, **131**, 384-411.
- Janjić, Z.I., 1994: The step-mountain eta coordinate model: Further developments of the convection, viscous sublayer, and turbulence closure schemes. *Mon. Wea. Rev.*, **122**, 927-945.
- Joussaume, S. and K.E. Taylor, 1995: Status of the Paleoclimate Modeling Intercomparison Project (PMIP). *Proc., First Int. AMIP Sci. Conf.*, Monterrey, CA, WCRP-92, 425-430.
- Kageyama, M., P.J. Valdes, G. Ramstein, C. Hewitt, and U. Wyputta, 1998: Northern Hemisphere storm tracks in present day and last glacial maximum climate simulations: A comparison of the European PMIP models. *J. Climate*, **12**, 742-760.
- Kiehl, J.T., J.J. Hack, G.B. Bonan, B.A. Boville, D.L. Williamson and P.J. Rasch, 1998: The National Center for Atmospheric Research Community Climate Model: CCM3. *J. Climate*, **11**, 1131-1149.
- Kutzbach, J.E. and P.J. Guetter, 1986: The influence of changing orbital parameters and surface boundary conditions on climate simulations for the past 18,000 years. *J. Atmos. Sci.*, **43**, 1726-1759.
- Kutzbach, J.E., R. Gallimore, S. Harrison, P. Behling, R. Selin and F. Laarif, 1998: Climate and biome simulations for the past 21,000 years. *Quat. Sci. Rev.*, **17**, 473-506.
- Manley, W.F. and D.S. Kaufman, 2002: *Alaska PaleoGlacier Atlas: Institute of Arctic and Alpine Research (INSTAAR)*, University of Colorado, http://instaar.colorado.edu/QGISL/ak_paleoglacier_atlas, v. 1.
- Meyers, M.P., P.J. DeMott and W.R. Cotton, 1992: New primary ice-nucleation parameterizations in an explicit cloud model. *J. Appl. Meteor.*, **31**, 708-721.
- Mix, A.C., E. Bard and R. Schneider, 2001: Environmental processes of the ice age: land, oceans, glaciers (EPILOG). *Quat. Sci. Rev.*, **20**, 627-657.
- Petit, J.R. and coauthors, 1999: Climate and atmospheric history of the past 420,000 years from the Vostok ice core, Antarctica. *Nature*, **399**, 429-436.
- Pollard, D. and S.L. Thompson, 1997: Climate and ice-sheet mass balance at the last glacial maximum from the Genesis Version 2 Global Climate Model. *Quat. Sci. Rev.*, **16**, 841-863.
- Rind, D., 1987: Components of the ice age circulation. *J. Geophys. Res.*, **92**, 4241-4281.
- Roe, G.H. and R.S. Lindzen, 2001: The mutual interaction between continental-scale ice sheets and atmospheric stationary waves. *J. Climate*, **14**, 1450-1465.
- Toracinta, E.R., R.J. Oglesby, and D.H. Bromwich, 2003: Atmospheric response to modified CLIMAP ocean boundary conditions during the Last Glacial Maximum. *J. Climate*, submitted.
- Tzeng, R.-Y., D.H. Bromwich, and T.R. Parish, 1993: Present-day climatology of the NCAR Community Climate Model Version 1. *J. Climate*, **6**, 205-226.
- Williams, J.W., W.I. Thompson, P.H. Richard and P. Newby, 2000: Late Quaternary biomes of Canada and the eastern United States. *J. Biogeog.*, **27**, 585-607.
- Wright, H.E., Jr., J.E. Kutzbach, T. Webb, W.F. Ruddiman, F.A. Street-Perrot and P.J. Bartlein, 1993: *Global climates since the last glacial maximum*. University of Minnesota Press, 544 pp.
- Yen, Y.C., 1981: Review of thermal properties of snow, ice, and sea ice. CRREL Rep. 81-10, 27 pp.